

# SUPPORTING INFORMATION

## The histone demethylase JMJD2B regulates endothelial-to-mesenchymal transition

Simone F. Glaser<sup>a,b,c</sup>, Andreas W. Heumüller<sup>a,b,c</sup>, Lukas Tombor<sup>a,b</sup>, Patrick Hofmann<sup>a,b</sup>, Marion Muhly-Reinholz<sup>a</sup>, Ariane Fischer<sup>a</sup>, Stefan Günther<sup>b,d</sup>, Karoline E. Kokot<sup>e</sup>, David Hassel<sup>f,b</sup>, Sandeep Kumar<sup>g</sup>, Hanjoong Jo<sup>g,h</sup>, Reinier A. Boon<sup>a,b</sup>, Wesley Abplanalp<sup>a,b</sup>, David John<sup>a,b</sup>, Jes-Niels Boeckel<sup>a,e,1</sup> and Stefanie Dimmeler<sup>a,b,1,2</sup>

<sup>a</sup>Institute for Cardiovascular Regeneration, Goethe University, 60590 Frankfurt, Germany;

<sup>b</sup>German Center of Cardiovascular Research (DZHK), Partner Site Rhine/Main 60439 Frankfurt, Partner Site Rhine/Main 61231 Bad Nauheim, Heidelberg/Mannheim 69120 Heidelberg, Germany;

<sup>c</sup>Faculty for Biological Sciences, Goethe University, 60590 Frankfurt, Germany;

<sup>d</sup>Cardiopulmonary Institute (CPI), Bioinformatics and Deep Sequencing Platform, Dept. I, Max Planck Institute for Heart and Lung Research, 61231 Bad Nauheim, Germany;

<sup>e</sup>Klinik und Poliklinik für Kardiologie, Universitätsklinikum Leipzig, 04103 Leipzig, Germany;

<sup>f</sup>Division of Cardiology, Department of Internal Medicine III, University Hospital Heidelberg, 69120 Heidelberg, Germany;

<sup>g</sup>Wallace H. Coulter Department of Biomedical Engineering, Emory University, Georgia Institute of Technology, Atlanta, GA 30322;

<sup>h</sup>Division of Cardiology, Emory University, Atlanta, GA 30322

<sup>2</sup>Corresponding author contacts:

Stefanie Dimmeler, PhD

Institute for Cardiovascular Regeneration, Center of Molecular Medicine, Goethe University

Theodor Stern Kai 7

60590 Frankfurt am Main

dimmeler@em.uni-frankfurt.de

Phone: +49-69-6301-6667

Fax: +49-69-6301-83462

<sup>1</sup>These authors contributed equally to this work

## Figure Legends

**S1. Regulation of JMJD2B by EndMT promoting stimuli in vivo.** RNA sequencing of partial carotid artery model (non ligated = right carotid artery, ligated = left carotid artery). Expression levels of Sm22 and Col3a1 of mice are depicted as FPKM values (n=3). Data are depicted as mean  $\pm$ SEM. Statistical significance was determined Student's t-test, \*P<0.05.

**S2. Knockdown of JMJD2B using siRNA and CRISPR-Cas9.** (A-H) HUVECs were treated either with siRNAs/gRNAs/inhibitor targeting JMJD2B or control (siScr) siRNA/gRNAs/DMSO. Data are represented as fold to siScr Ctrl. (A) SM22 mRNA using human microarray of ECs treated with siRNAs and incubated under EndMT conditions (N=3). (B) Representative images of Vimentin IF. Nuclei in blue, Vimentin in red (Scale bar=50  $\mu$ m). (C) Quantification of Vimentin staining (N=3) (D) SM22 mRNA after different siRNAs (a-c), followed by EndMT, analyzed by RT-qPCR norm. to RPLP0 (N=5). (E) Knockdown using the CRISPR-Cas9 technology. Protein of JMJD2B was quantified via western blot (n=5). (F) Protein level of CDH5 by measuring the intensity of IF stainings 92h after knockdown (n=3). (G) SM22 mRNA determined by RT-qPCR after siRNA, followed by EndMT and additional incubation in 1% O<sub>2</sub> (hypoxia) or 21% O<sub>2</sub> (normoxia), norm. to RPLP0 (N=3). (H) SM22 mRNA after inhibitor treatment in final concentrations of 1, 5 and 10  $\mu$ M, determined by RT-qPCR. DMSO was used as Ctrl, norm. to RPLP0 mRNA ( $2^{-\Delta Ct}$ , n=4). Data are depicted as mean  $\pm$ SEM. Statistical significance was determined using Student's t-test or Mann-Whitney-U-Test; \*P<0.05.

**S3. Regulation of JMJD2B by EndMT promoting stimuli in vitro.** (A-F) HUVECs were treated with siRNA Ctrl or siRNA targeting JMJD2B (siJMJD2B) and incubated accordingly to the TGF- $\beta$ 2 induced EndMT protocol. Data are depicted as violin plots (A-C) and as percentage of all cells (D-F) for single cell sequencing expression levels (UMI>0) of mesenchymal markers. siScr Ctrl in grey, siScr EndMT in red and siJMJD2B EndMT in black. Statistical significance was determined by bimodal maximum likelihood test (A-C) or Chi-Square test with Yates correction (D-F) \*P<0.05.

**S4. Knockdown of JMJD2B using siRNA and its effect on TGF- $\beta$ 1 and IL-1 $\beta$  driven EndMT.** (A-E) HUVECs were treated either with siRNAs targeting JMJD2B or control (siScr) siRNA, followed by EndMT induction by TGF- $\beta$ 1 and IL-1 $\beta$ . mRNAs were determined by RT-qPCR, normalized to RPLP0. Data are represented as fold to siScr Ctrl (n=5). mRNA levels of (A) ZEB2, (B) CD44, (C) NOS3 and (D) CD34. IF-staining of (E) PDGFR $\beta$  in red, CDH5 in green and nuclei in blue (scale bar = 10 $\mu$ m). Data are depicted as mean  $\pm$ SEM. Statistical significance was determined using Student's t-test; \*P<0.05.

**S5. Regulation of EndMT marker genes and functional effects in Jmjd2b<sup>IEC-KO</sup> hearts.** (A) Boxplot of single-cell data comparing expression of mesenchymal genes in all cells in Ctrl (grey) vs. Jmjd2b<sup>IEC-KO</sup> (red) 3 days post-AMI. Significance levels of Bonferroni adjusted p-values: \* p<0.05, \*\* p<1x10<sup>10</sup>, \*\*\* p<1x10<sup>35</sup>. (B-C) Functional effects of Jmjd2b<sup>IEC-KO</sup> measured by ejections fraction (EF) and cardiac fibrosis. Mice were treated as shown and described in Fig. 3. (B) EF was analysed using the Simpson method and measured on day 0 (d0), day 7 (d7) and day 14 (d14) post-AMI. Values are depicted as % (n=7-10). (C) Cardiac fibrosis was measured using the intensity of Sirius red, normalized to total area of the section 14 days post-AMI (n=7-10, with 3 sections/heart). Data are depicted as mean  $\pm$  SEM.

**S6. JMJD2B did not change global histonemethylation pattern.** (A) Representative immunoblot of global H3K4me3 and H3K9me3 after knockdown of JMJD2B followed by EndMT induction of HUVECs. Histone H3 served as a loading control. (B) Densitometric

analysis of the immunoblots, normalized to protein level of histone H3 (N=4). Data are depicted as mean  $\pm$ SEM.

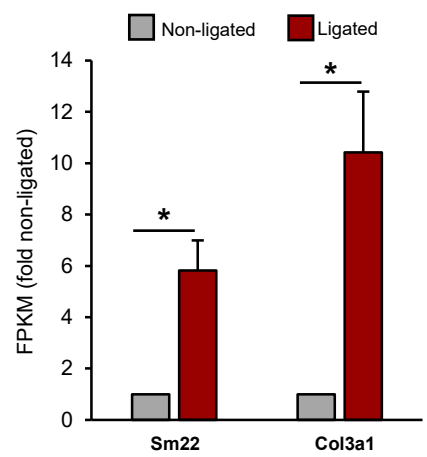
**S7. H3K9me3 Peaks.** (A) Detailed annotation of highest H3K9me3 peaks. The highest H3K9me3 peaks from ChIP-seq were analyzed in detail using UCSC Genome Browser (Version: human Dec. 2013 (GRCh38/hg38) assembly and Repeat Masker program of Arian Smit on GRCh38.p12 version). (B-F) Illustration of H3K9me3 ChIP-seq peak location of ACTB (B) CNN1 (C), SULF1 (D), AKT3 (E) and TGF- $\beta$ 2 (F).

**S8. Validation of genes regulated on H3K9me3 level upon EndMT and bioinformatical analysis of the role of JMJD2B on EndMT.** (A-B) RNA Sequencing of HUVECs underwent EndMT as described above (n=4). (A) Data are depicted as mean  $\pm$ SEM. Statistical significance was determined to Ctrl respectively using Student's t-test; \*P<0.05. (B) Heatmap represents the top 50 significant upregulated genes upon EndMT. The highest values are depicted in red, the lowest in blue. (C) KEGG-pathway analysis of significantly downregulated genes after siJMJD2B and EndMT treatment (microarray analysis). (D) Venn-diagram of genes showing overlap of significantly downregulated H3K9me3 peaks under EndMT conditions in ChIP-sequencing and genes which are significantly downregulated after siJMJD2B in EndMT undergoing HUVECs (micro-array analysis). (E) GAD-Disease analysis of genes included in described overlay of (D).

**S9. Effect of AKT3 on EndMT.** mRNA expression level of (A) SM22 and (B) CNN1 after siRNA-mediated knockdown of AKT3 followed by EndMT induction (n=4). Data are depicted as mean  $\pm$ SEM. Statistical significance was determined to Ctrl respectively using Student's t-test; \*P<0.05.

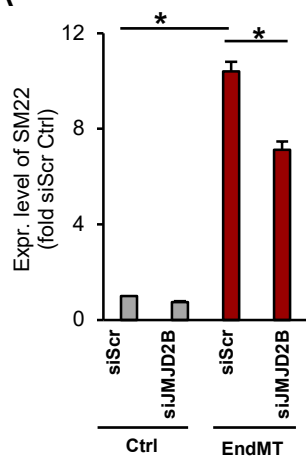
# Supporting Information 1

A

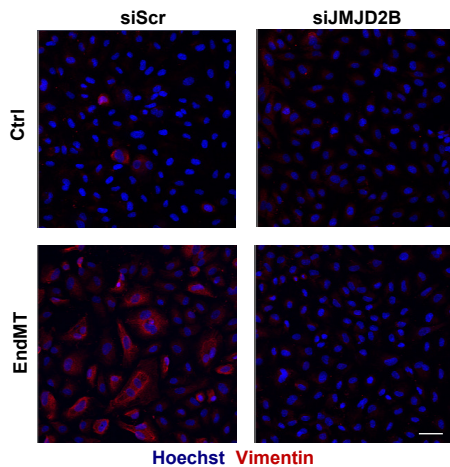


# Supporting Information 2

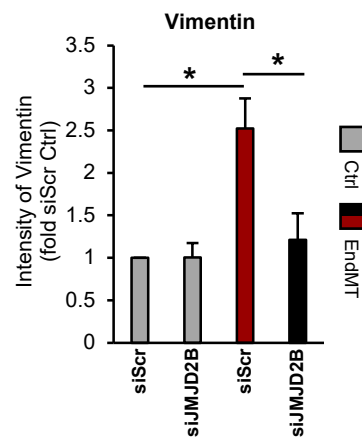
## A



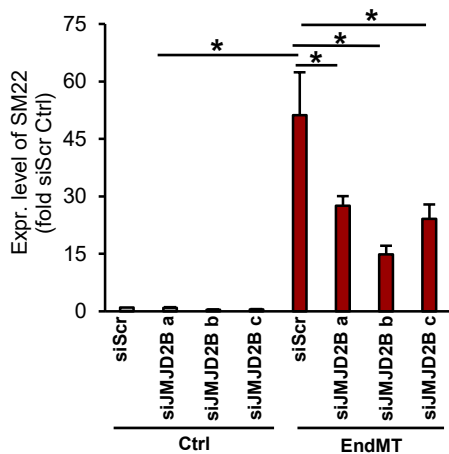
## B



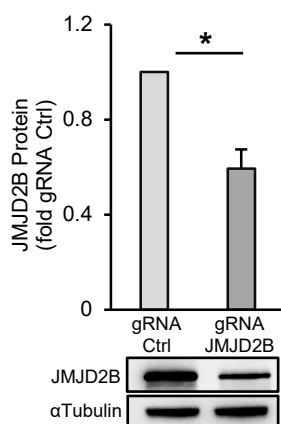
## C



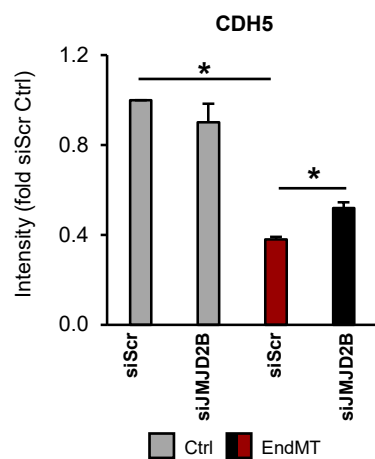
## D



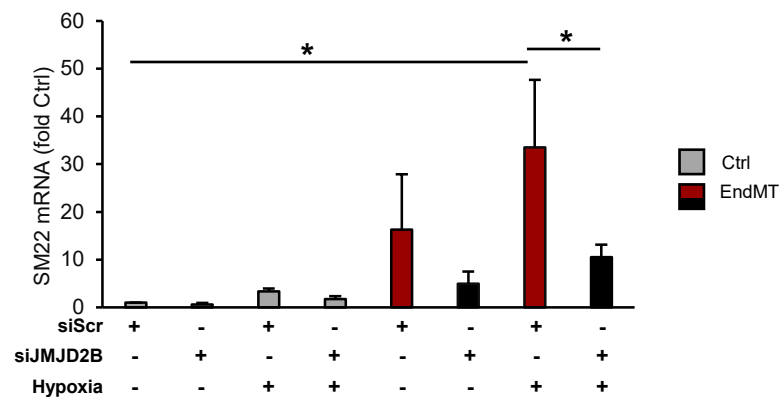
## E



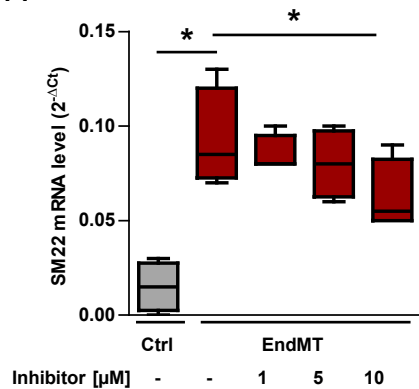
## F



## G

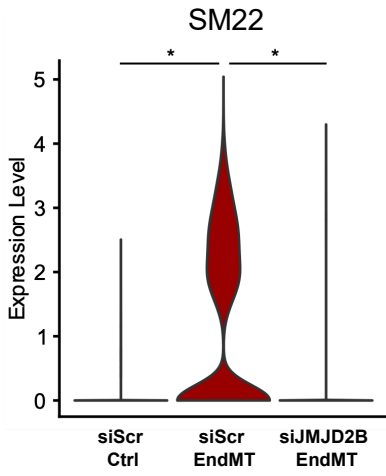


## H

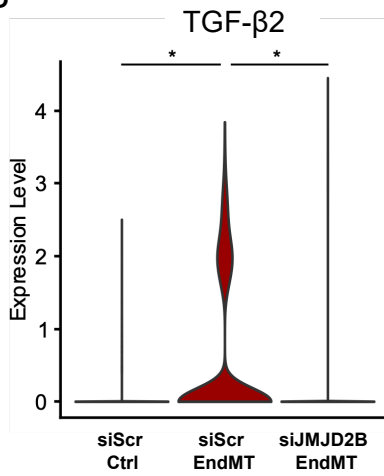


# Supporting Information 3

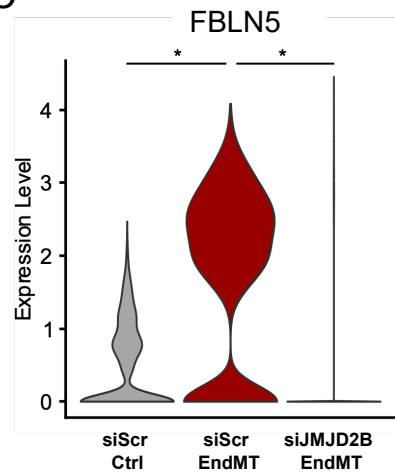
**A**



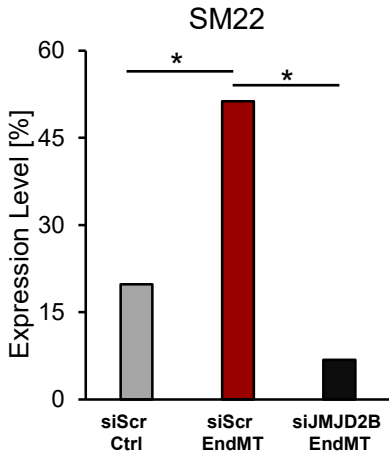
**B**



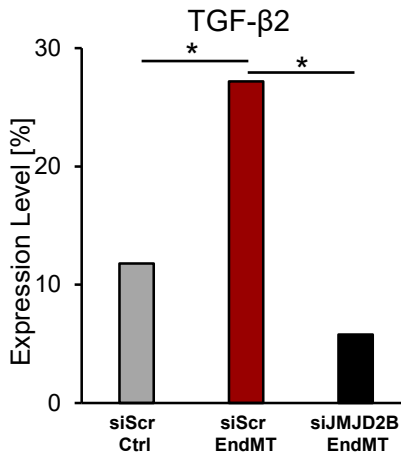
**C**



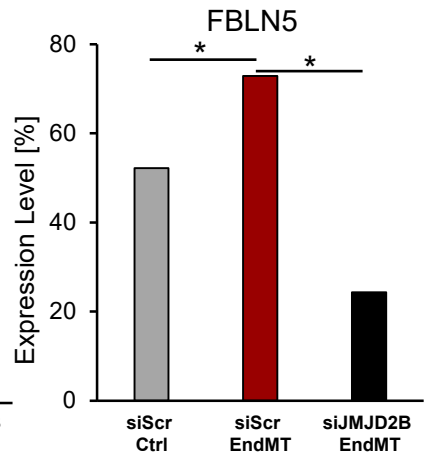
**D**



**E**

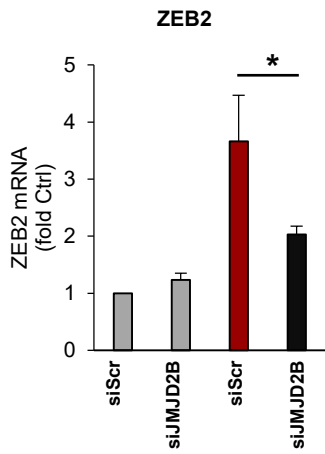


**F**

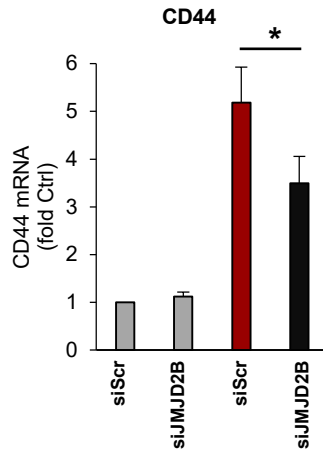


# Supporting Information 4

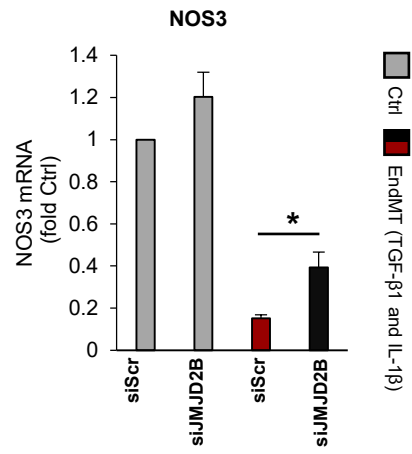
**A**



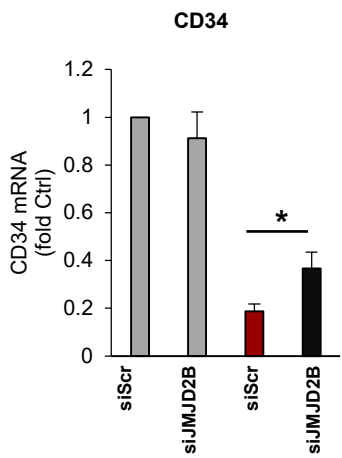
**B**



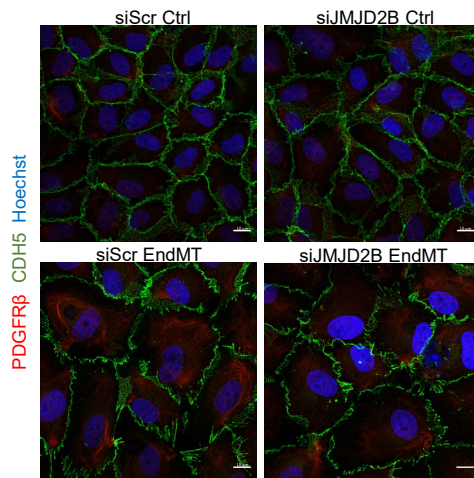
**C**



**D**

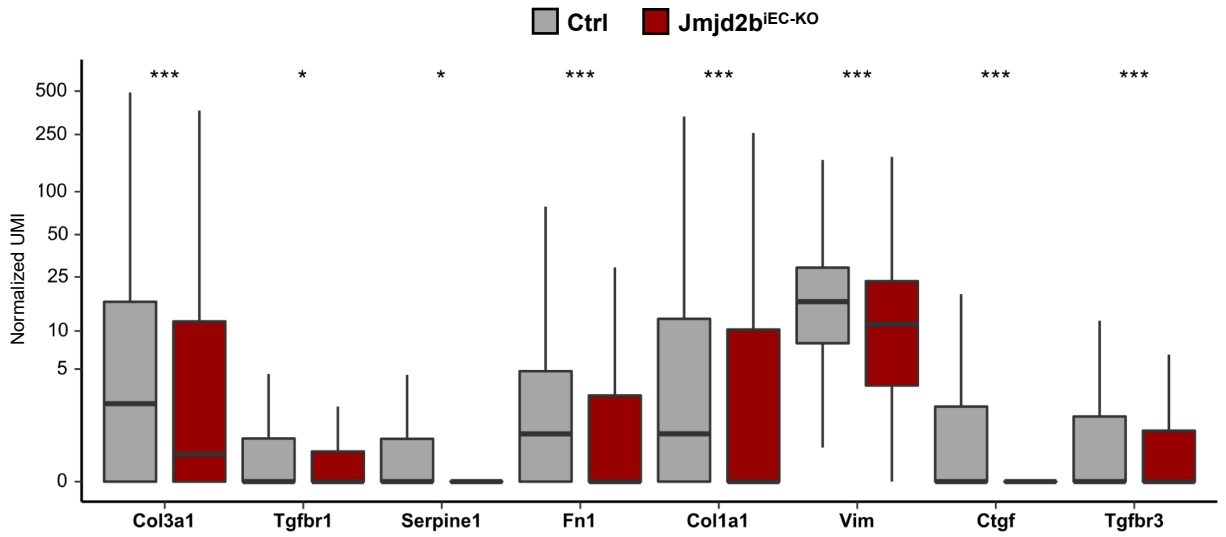


**E**

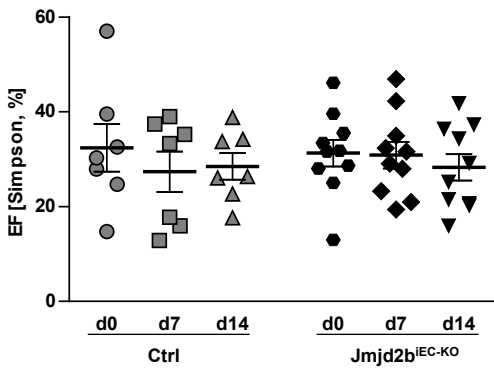


# Supporting Information 5

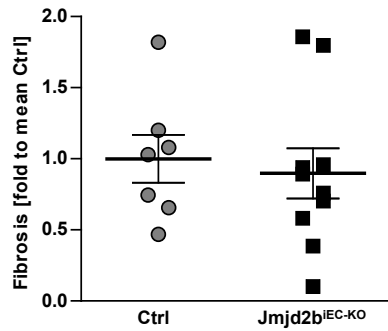
## A



## B



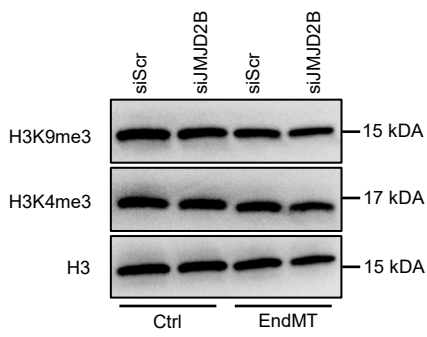
## C



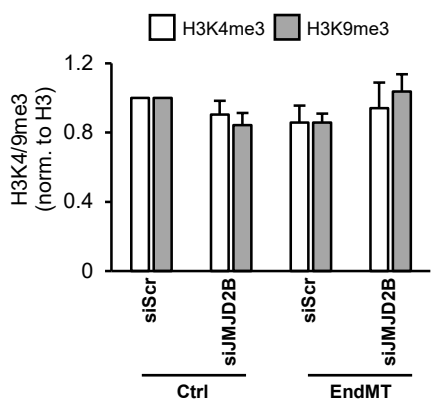


# Supporting Information 6

## A



## B



# Supporting Information 7

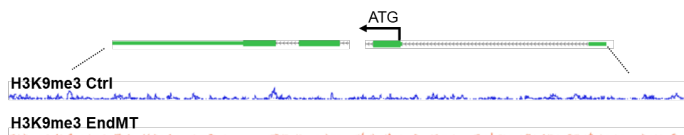
A

## H3K9me3 Methylation Peaks

Chr.	Start	End	Value	Near gene (-10 kB)	Location	Detailed annotation	
Ctrl	hs12	132925395	132926791	171	ZNF605, exon 1	Close to telomere chromosome 12, band: 12q24.33	
	hs8	144975145	144976702	122	ZNF252P (pseudogene, exon)	outer chromosome 8, band: 8q24.3	A-rich repeat
EndMT	hs5	49600288	49601774	877		Band: 5q11.1. in the centromere	satellite DNA-region
	hs20	31073518	31074724	275		Band: 20q11.21 near the centromere	simple repeats
	hs10	41890059	41891851	235		Band: 10q11.21 near the centromere	simple repeats
	hs10	41883449	41884467	201		Band: 10q11.21 near the centromere	simple repeats
	hs10	41874669	41876112	131		Band: 10q11.21 near the centromere	simple repeats
	hs21	10429807	10430813	118	BAGE2 intron	Band: 21p11.2	Repeat MER20. family hAT-Charlie. repeat L2a. family L2
	hs4	49109720	49110955	104		Band: 4p11 in the centromere	satellite DNA-region
hs4	49635305	49637223	83		Band: 4p11 in the centromere	satellite DNA-region	

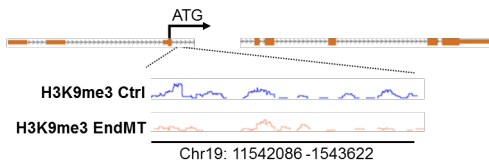
B

ACTB Chr7: 5527152-5530603



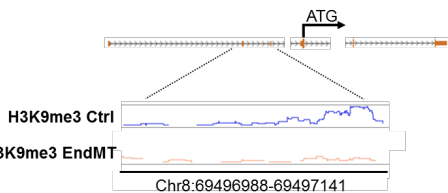
C

CNN1 Chr19:11538767-11550322



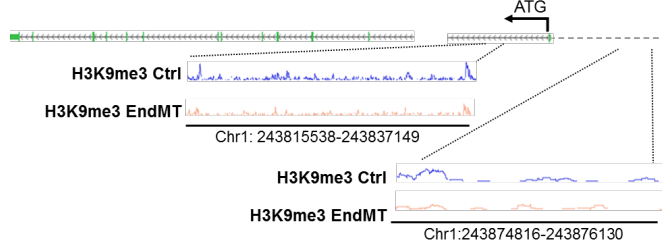
D

SULF1 Chr8:69466624-69660915



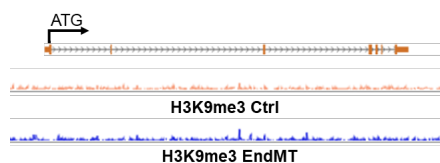
E

AKT3 Chr1:243488233-243851079



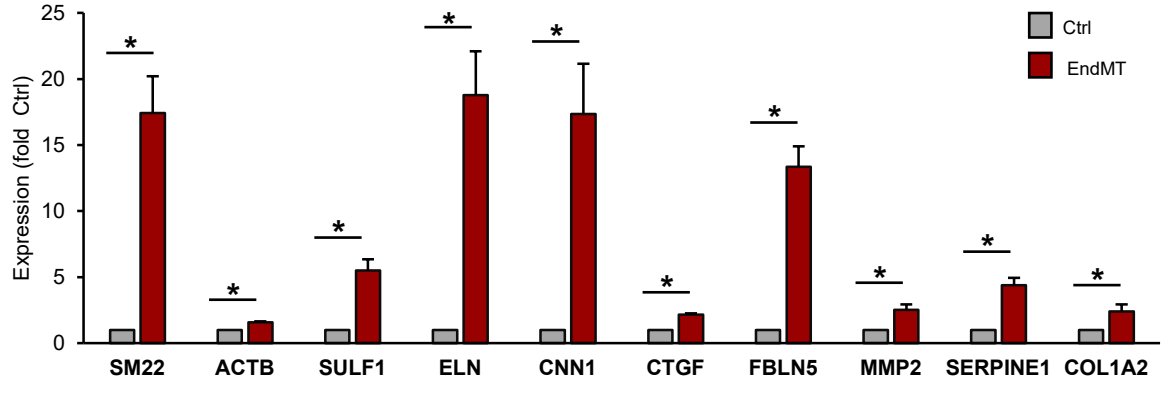
F

TGF-β2 Chr1: 218345228-218443925

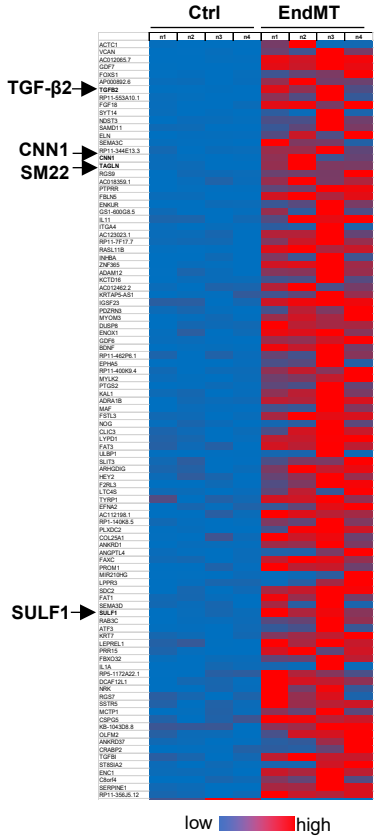


# Supporting Information 8

A



B



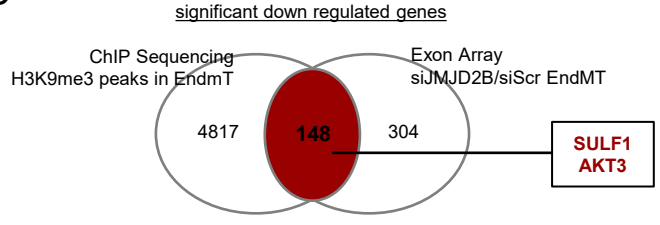
C

EndMT related pathways	Regulated Genes	p-value
MAPK signaling pathway	18	9.7E-5
Focal adhesion	12	9.3E-3
Rap1 signaling pathway	12	1.1E-2
Regulation of actin cytoskeleton	12	1.1E-2
Ras signaling pathway	12	1.8E-2
Hippo signaling pathway	8	6.6E-2

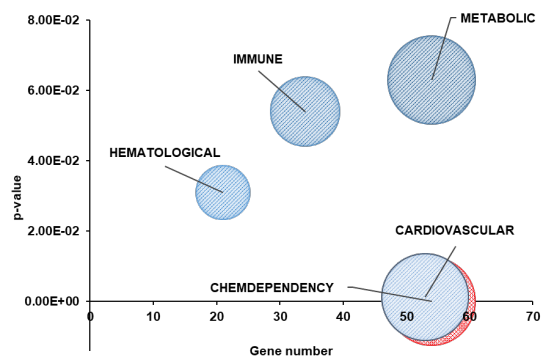
  

AKT3	MAP4K4
ELK4	NRAS
GNG12	PLA2G4A
RAP1A	PPP3R1
RAPGEF2	PTPRR
CACNA2D1	RPS6KA5
HSPA2	STK4
LAMTOR3	ZAK
MAP3K7	TGF-β2

D

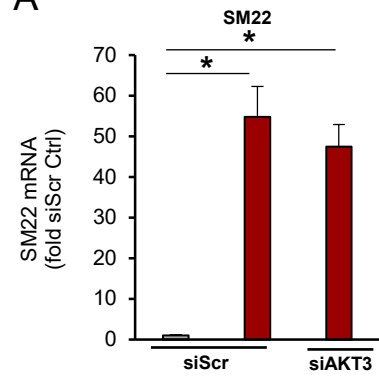


E

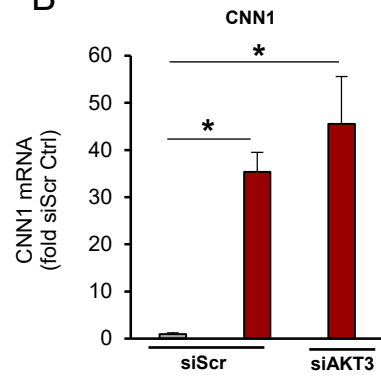


# Supporting Information 9

A



B



Ctrl EndMT

## SUPPORTING INFORMATION

### Detailed methods

#### Cell culture of HUVECs

Experiments were performed using human umbilical vein endothelial cells (HUVECs) purchased from Lonza. Cells were cultured in endothelial basal medium without phenol red (#C-22215, PromoCell), supplemented with hydrocortisone (#CC-4035C, Lonza), ascorbic acid (#CC-4116C, Lonza), bovine brain extract (#CC-4092C, Lonza), epidermal growth factor (#CC-4017, Lonza), 10% fetal bovine serum (FBS) (#CC-4101, Lonza) and Gentamicin+Amphotericin-B -1000 (#CC-4081C, Lonza).

#### Endothelial-to-mesenchymal transition assay

For the EndMT assay two distinct media were used referred to as either full medium ("Ctrl") or differentiation media ("DM"). The composition of the media is listed in the table below. For the assay,  $4 \times 10^5$  HUVEC were seeded in a 60 mm cell culture dish. After 24<sup>h</sup>, cells were incubated in Ctrl media or DM with either 10 ng/ml TGF- $\beta$ 2 (referred as "EndMT", #302-B2, R&D System) or 10 ng/ml TGF- $\beta$ 1 (#240-B, R&D System) and/or 10 ng/ml IL-1 $\beta$  (#200-01B, Peprotech). After additional 48 h of incubation, the treatment was repeated. After a total of 96 h, RNA was isolated.

#### Cell culture and differentiation media:

Medium	Component	Catalogue	Company
Endothelial full medium ("Ctrl")	Endothelial cell basal medium (phenol red-free)	C-22215	PromoCell
	10% FBS	4133	Invitrogen
	Hydrocortisone	CC-4035C	Lonza
	Gentamycin+Amphotericin-B	CC-4081C	Lonza
	Ascorbic acid	CC-4116C	Lonza
	EGF	CC-4017C	Lonza
	BBE	CC-4092C	Lonza
Endothelial differentiation medium ("DM")	Endothelial cell basal medium (phenol red-free)	C-22215	PromoCell
	10% FBS	4133	Invitrogen

	Hydrocortisone	CC-4035C	Lonza
	Gentamycin+Amphotericin-B	CC-4081C	Lonza
	Ascorbic acid	CC-4116C	Lonza

### **JMJD2B inhibitor treatment**

Cells were treated either with Ctrl media or DM including TGF- $\beta$ 2 as described above. Additionally, a final concentration of 1, 5 or 10  $\mu$ M Inhibitor (CCT365599) or DMSO as a control was added to the medium.<sup>1</sup> Final concentration of DMSO was 0.1% in all samples. CCT365599 was provided by Prof. Julian Blagg, Cancer Research UK Cancer Therapeutics Unit at the Institute of Cancer Research, London, UK.

### **Hypoxia exposure of endothelial cells**

4 x 10<sup>5</sup> HUVECs were incubated 24 h after seeding in 60 mm cell culture dishes for 24 h under hypoxic conditions (1 % or 0.2 % O<sub>2</sub>, 37°C) or normoxic conditions (21% O<sub>2</sub>, 37°C). For hypoxia experiments in combination with EndMT treatment, HUVECs were stimulated either with Ctrl media or DM including TGF- $\beta$ 2 as described above and immediately incubated under hypoxic (1% O<sub>2</sub>, 37°C) or normoxic conditions 24 h after seeding. After additional 72 h RNA was isolated.

### **RNA analysis**

Total RNA was isolated using Qiazol Lysis Reagent (#79306; Qiagen) and miRNeasy-kit (#217004; Qiagen) with additional DNase I (#79254; Qiagen) digestion according to the manufacturer's protocol. 1 $\mu$ g of RNA from each sample was reverse-transcribed using random hexamer primers (10 min at 25°C, 15 min at 42°C, 5 min at 99°C) by MMLV Reverse Transcriptase (#N8080018; Life technologies) as previously described.<sup>2</sup> For RT-qPCR, cDNA was amplified using Fast SYBR Green Mastermix (#4385612 Life Technologies) on a ViiA7- Realtime qPCR System (Life Technologies). Expression levels of mRNAs were normalized to the housekeeping genes RPLP0 or GAPDH, using the 2<sup>- $\Delta$ Ct</sup> method. The primer sequences used in RT-qPCR are listed in the table below.

SYBR Green PCR primer:

Primer name	Sequences (5'->3')	Target gene	Species
RPLP0-fw	GGCGACCTGGAAGTCCAACCT	RPLP0	human
RPLP0-rv	CCATCAGCACCCACAGCCTTC	RPLP0	human
SULF1-fw	AGATCTCCAGGCTTCCAGTG	SULF1	human
SULF1-rv	GGTACAGTTCTCTCTCACAAATGG	SULF1	human
SM22-fw	AAGAATGATGGGCACTACCG	TAGLN	human
SM22-rv	ATGACATGCTTTCCCTCCTG	TAGLN	human
CNN1-fw	CTGGCTGCAGCTTATTGATG	Calponin	human
CNN1-rv	CTGAGAGAGTGGATCGAGGG	Calponin	human
JMJD2B-fw	GGCTCCTACAGCGACAACCT	JMJD2B	human
JMJD2B-rv	CCAGCTGGACACAGTCCCTACT	JMJD2B	human
TGF- $\beta$ 2-fw	TTGCAGAACCCAAAAGCCAG	TGF- $\beta$ 2	human
TGF- $\beta$ 2-rv	TCACAACCTTTGCTGTGCGATGT	TGF- $\beta$ 2	human
AKT3-fw	AACGACCAAAGCCAAACACA	AKT3	human
AKT3-rv	AGCTTCTGTCCATTCTTCCCT	AKT3	human
$\beta$ -actin-fw	AGAGGGAAATCGTGCGTGAC	$\beta$ -actin	human
$\beta$ -actin rv	CAATAGTGATGACCTGGCCGT	$\beta$ -actin	human
ZEB2-fw	CGCACATCAGCAGCAAGAAA	ZEB2	human
ZEB2-rv	ACCCGTGTGTAGCCATAAGA	ZEB2	human
CD44-fw	GCATCGGATTTGAGACCTGC	CD44	human
CD44-rv	CAGATGGAGTTGGGGTGGAT	CD44	human
NOS3-fw	GTGGTAACCAGCACATTTGG	NOS3	human
NOS3-rv	AGGACACCAGTGGGTCTGAG	NOS3	human
CD34-fw	GCAAGCCACCAGAGCTATTC	CD34	human
CD34-rv	AATAGCCAGTGATGCCCAAG	CD34	human
GAPDH-fw	ATGGAAATCCCATCACCATCTT	GAPDH	human
GAPDH-rv	CGCCCCACTTGATTTTGG	GAPDH	human
CNN1-ChIP-fw	ACCCGCCTTAGTCTCACAAA	Calponin	human

CNN1-ChIP-rv	ATGAGGTTTTGAGGCGAGGA	Calponin	human
AKT3-ChIP-fw	AGCCTGTAATCCCAGCACTC	AKT3	human
AKT3-ChIP-rv	AGGCTGACCTTGACGTCCT	AKT3	human
SULF1-ChIP-fw	CCAAGGTGACGGAAGCTAAAACAG	SULF1	human
SULF1-ChIP-rv	GCCTAGGTGACAGATCAAGACTCTGTC	SULF1	human
mJmjd2b-fw	CGGTGGACAGACGGTAATCT	Jmjd2b	mouse
mJmjd2b-rv	AGCTGAGACCCATCCTCAA	Jmjd2b	mouse
m18srRNA-fw	AGGAATTGACGGAAGGGCACCA	18s rRNA	mouse
m18srRNA-rv	GTGCAGCCCCGGACATCTAAG	18s rRNA	mouse
mRplp0-fw	TTTGACAACGGCAGCATTTA	Rplp0	mouse
mRplp0-rv	CCGATCTGCAGACACACT	Rplp0	mouse

### **CRISPR-Cas9-based knockdown of JMJD2B**

The backbone plasmid pLenti CRISPRV2-GFP plasmid (#82416, Addgene) was kindly provided from Manuel Kaulich, Frankfurt. The used guide RNAs were designed using GPP-web portal (<https://portals.broadinstitute.org/gpp/public/>), based on the KDM4B-201 ENST00000159111.8 transcript

gRNA#1\_fw: **CACCG**ATGTCATCATACGTCTGCCG

gRNA#1\_rv: **AAACCGGCAGACGTATGATGACATC**

gRNA#2\_fw: **CACCGTGGCCTACATAGAGTCGCA**

gRNA#2\_rv: **AAACTGCGACTCTATGTAGGCCAC**

gRNA#3\_fw: **CACCGCATGACGTTTCGCCCAACCA**

gRNA#3\_rv: **AAACTGGTTGGGCGAAACGTCATGC**

Lentivirus stocks were produced in HEK293T cells using pCMVΔR8.91 as packaging plasmid and pMD2.G (Addgene #12259). Empty backbone-vectors were used as control. HUVECs were transduced, followed by EndMT induction as described before. RNA and Protein were isolated after 96 h and analyzed by qRT-PCR or Westernblot.

### **Small interfering RNA knockdown**

For siRNA-mediated gene silencing,  $4 \times 10^5$  HUVEC were seeded in a 60 mm cell culture dish. After 24 h, cells were transfected with GeneTrans II (#0203B Mobitec) as



described previously using siRNA pools or single sequences listed in the table below.<sup>2</sup> EndMT and hypoxia treatment were started 24 h after transfection as described above.

SiRNA pools and sequences:

siRNA name	Catalogue #	Company
siScr-pool	L-004290-00-0020	Dharmacon
siJMJD2B-pool	D-001810-10-20	Dharmacon

siRNA name	Sequences (5'->3')	Company
siScr	GUGGGCACCGAUAUCUUGA	Sigma
siJMJD2B a	UGAUGCUCUCAGGGUACAG	Sigma
siJMJD2B b	GGCAUAAGAUGACCCUCAU	Sigma
siJMJD2B c	CAAUACGUGGCCUACAUA	Sigma
siSULF1	ACUUAUCACUAACGAGA	Sigma
siAKT3	GCACACACUCUCUAACUGAAA	Sigma

**Immunofluorescence**

1.53 x 10<sup>4</sup> HUVECs were seeded into 8-chamber glass slides (#177402, Thermo Fisher), coated with 1 µg/ml human fibronectin (#F0895 Sigma Aldrich). Cells were transfected with siRNAs and cultivated as previously described.<sup>3</sup> After 96 h cells were fixed in 4 % PFA and permeabilized using 0.1% TritonX-100 followed by blocking with 10% donkey serum. The primary antibodies were incubated overnight at 4 °C, secondary antibodies for 1 h at RT. Nuclei were stained using DAPI Mounting Medium (#H-1200 Vector). Imaging was done using Zeiss Observer.Z1 microscope.

Antibodies for Immunofluorescence:

Antibody	Species	Concentration	Catalog no.	Company
Anti-CDH5	rabbit	1:200	#2500S	Cell signalling
Anti-SM22	goat	1:100	#ab10135	Abcam
Anti-Vimentin	goat	1:40	#AB1620	Millipore
Anti-PDGFRβ	rat	1:100	#14-1402-82	Invitrogen

Anti-goat-555	donkey	1:200	#ab150130	Abcam
Anti-rabbit-488	donkey	1:200	#A-21206	Life technologies
Anti-rat-594	donkey	1:200	#A-21209	Life technologies

### **Immunoblot analysis**

Proteins were isolated using RIPA buffer (#R0278, Sigma Aldrich) containing protease-inhibitor cocktail (#11852700, Roche). Histones were isolated using Histone extraction Kit (#ab113476, Abcam). 10 or 30 µg of the proteins were separated using SDS-PAGE and transferred on to nitrocellulose membranes or methanol activated PVDF membrane using a semi-dry or wet blot (1.5 h, 80 V) transfer. The membranes were blocked for 1 h with 5% skim milk or 5 % BSA in Tris-buffered saline supplemented with 0.05 % Tween-20 and incubated with the antibodies listed in the table below. Proteins were detected based on HRP substrate-based enhanced chemiluminescence (#WBKLS0500, Millipore).

### **Antibodies for Immunoblot:**

<b>Antibody</b>	<b>Species</b>	<b>Concentration</b>	<b>Catalog no.</b>	<b>Company</b>
Anti-SM22	rabbit	1:1000	ab14106	Abcam
Anti-JMJD2B	rabbit	1:1000	ab191434	Abcam
Anti-GAPDH	rabbit	1:1000	21118	Cell signalling
Anti-β-ACTIN	rabbit	1:1000	4970	Cell signalling
Anti-Tubulin	rat	1:5000	ab6160	Abcam
Anti-Topoisomerase I	mouse	1:1000	556597	BD Pharmingen
H3K4me3	rabbit	1:1000	ab8580	Abcam
H3K9me3	rabbit	1:1000	ab176916	Abcam
H3	goat	1:500	ab12079	Abcam
Anti-JMJD2B (for CRISPR-Cas)	rabbit	1:1000	ab191434	Abcam
Anti-rabbit	donkey	1:1000	ab6802	Abcam
Anti-goat	donkey	1:3000	ab97110	Abcam
Anti-rat	donkey	1:5000	ab102265	Abcam

Anti-mouse	donkey	1:5000	ab97030	Abcam
------------	--------	--------	---------	-------

### **In vitro analysis of vascular dismantling**

After EndMT induction, vascular gaps were analyzed by CDH5 staining (Staining procedure is described in the immunofluorescence section) of differentiated endothelial cell with or without siRNA transfection. For each condition, five random fields were analyzed per replicate. Furthermore, permeability was analysed by adding fluorescein isothiocyanate–conjugated Dextran ( $2 \times 10^6$ , #52471 Sigma Aldrich) to the cells growing on fibronectin-coated inserts (1  $\mu$ m pore size, #6662610 Greiner). Fluorescent signal in the bottom well was measured with the Glomax (Promega) after 30min of incubation.

### **In vitro analysis of CDH5 protein level**

After EndMT treatment of seven days, the intensity of the CDH5 staining was measured with ImageJ (staining procedure is described in the immunofluorescence section). For each condition, five random fields were analyzed per replicate.

### **In vitro analysis of SM22 positive cells**

After EndMT induction, SM22 positive cells were counted based on the SM22 staining (staining procedure is described in the immunofluorescence section). We distinguished between cells, which were negative for SM22, positive or showed an intermediate protein level. For each condition, 9-10 random fields were analyzed per replicate.

### **RNA- Sequencing**

RNA was isolated as described before. 900ng of total RNA was used as input for whole transcriptome RNA-seq library preparation (TruSeq® Stranded Total RNA, Illumina) following low throughput protocol. Sequencing was performed on Nextseq 500 (Illumina) using V2 chemistry and 75bp single-end setup. Raw reads (in average 44M per sample) were accessed for sequencing quality (adapter content, duplication rates) by FastQC (Andrews S. 2010, FastQC: a quality control tool for high throughput sequence data. Available online at: <http://www.bioinformatics.babraham.ac.uk/projects/fastqc>. Read alignment was performed with Star version 2.5.<sup>4</sup> against Ensembl human genome version GRCH38.79. Differentially expressed genes were identified using Cuffdiff2 version 2.1.1..<sup>5</sup> Genes differentially expressed were defined as those with >1.4-fold change and *P* value < 0.05 by Student *t* test. RNA expression levels under static and

laminar flow conditions determined by RNA sequencing was analyzed using published dataset (GSE54384).<sup>6,7</sup> RNA expression levels of *Jmjd2b* and several mesenchymal markers in partial carotid ligation operate male C57Bl/6 mice was performed by the laboratory of Prof. Hanjoong Jo (n=3-6).<sup>8</sup> Total RNA from intima was obtained from the LCAs and RCAs of mice sacrificed at 12 h and 48 h post ligation, as they described previously. The endothelial-enriched RNA samples from the RCAs and LCAs were depleted of ribosomal RNA by using NEBNext® rRNA Depletion Kit. Double-stranded cDNA libraries were prepared according to the Nugen Ovation RNA-seq system (Cat#7102-08) followed by Nugen Ovation Ultralow library system (Cat#0344-32); Input RNA: 1 ng each following manufacturer's instructions. The cDNA libraries were then sequenced on an Illumina 2000 HiSeq using v3 chemistry according to the Illumina Sequencing User's Guide (San Diego, CA); 50 million 100-bp paired-end reads were generated per library. Base calling and FASTQ were done with Illumina's HiSeq Control Software version 1.5.15.1 (RTA v1.13.18 and bclfastq v1.8.3). Sequenced reads were mapped to the mouse reference genome with TopHat version 2.0.5, and differentially expressed genes were assessed by use of Cuffdiff, a part of the Cufflinks version 2.1.1 package.

### **Microarray analysis**

RNA was isolated as described in the RNA isolation section. Gene-expression analysis was performed using the GeneChip Human Exon 1.0 ST array (#900651 Affymetrix) following the supplier's instructions. Data were analyzed by using the Exon Array Analyzer (EAA) Web interface (<http://eaa.mpi-bn.mpg.de/>).<sup>9</sup> Data were in depth bioinformatically analyzed using GO-panther, KEGG-pathway and GAD-disease analysis-tool.

### **Chromatin immunoprecipitation sequencing (ChIP-Seq)**

The ChIP Sequencing protocol was adapted from C. Schmidl *et al.* with the following changes.<sup>10</sup> HUVECs grown in T175 culture flask were washed with 10 ml PBS, detached using 2 ml Trypsin/EDTA and stopped using 8 ml EBM medium containing 10% FCS. Cell number was adjusted to  $4 \times 10^6$  cells (per IP) in 10 ml fresh EBM medium (10% FCS) and cross-linked with a final concentration of 1% formaldehyde for 10 min at room temperature. 1 ml glycine (1.25 M) was added and the suspension was

incubated for 5 min at room temperature to stop the fixation reaction. Cells were collected at 500 x g for 10 min at 4°C. Subsequently, cells were washed twice with ice-cold PBS containing 1µM PMSF+Protease Inhibitor. Next, 1 ml cell lysis buffer (HEPES (50 mM, pH 7.4), NaCl (140 mM), EDTA (1 mM), EGTA (0.5 mM), Glycerol (10% V/V), NP-40 (0.5% V/V), Triton-X100 (0.25% V/V), PMSF (1µM) 1x protease inhibitor cocktail (Sigma Aldrich)) was added to the pelleted cells and incubated for 10 min on ice. The nuclei were then pelleted by centrifugation at 1000 x g for 10 min at 4°C. The isolated nuclei were lysed with 150 µl nuclei lysis buffer (Tris-HCl (10 mM, pH 7.6), EDTA (1 mM), SDS (0.1% W/V) 1x protease inhibitor cocktail (Sigma Aldrich)) and split three ways into Covaris sonification tubes. Shearing was done in a Covaris S220 for 12 min with 2% Duty cycle, peak incident power of 105 Watts and 200 cycles per burst. The lysates were pooled and centrifuged at full speed for 5 min at 4°C. The supernatant containing the chromatin was collected. The volume was adjusted to 300 µl with IP buffer (HEPES (20 mM, PH7.4), NaCl (150 mM), EDTA (1 mM), SDS (0.1% W/V), EGTA (0.5 mM), Triton-X100 (1% V/V), and 2 µg of the H3K9me3 antibody (C15410193, Diagenode) or negative control IgG (12-371, Merck Millipore) was added followed by overnight incubation at 4°C with constant rotation. Protein A/G beads (C030200001, Diagenode; 40 µl beads per IP) were washed 3 x with 1 ml PBS. Next the chromatin-antibody-complex was added to the pelleted beads and incubated for 2 h at 4°C with constant rotation. The bead-antibody-chromatin complexes were now washed with the following wash buffers WB1 (20 mM HEPES, 150 mM NaCl, 0.1% SDS, 0.1% DOC, 1% Triton X-100, 1 mM EDTA, 0.5 mM EGTA) (twice), WB2 (20 mM HEPES, 500 mM NaCl, 0.1% SDS, 0.1% DOC, 1% Triton X-100, 1 mM EDTA, 0.5 mM EGTA) (once), WB3 (20 mM HEPES, 250 mM LiCl, 0.5% DOC, 0.5% NP-40, 1 mM EDTA, 0.5 mM EGTA) (once), and twice with WB4 (20 mM HEPES, 1 mM EDTA, 0.5 mM EGTA). Beads were then incubated with 70 µl elution buffer (0.5% SDS, 300 mM NaCl, 5 mM EDTA, 10 mM Tris-HCl pH 8.0) containing 2 µl of Proteinase K (CS203218, MerckMillipore) for 1 hour at 55°C and overnight at 65°C to reverse crosslinking. After centrifugation with 1000 x g for 5 min at room temperature the supernatant was transferred to a new tube. Next 31 µl of elution buffer containing Protease K was added to the beads for 1h at 55°C, and eluates were combined. DNA purification was done using MinElute Reaction Cleanup Kit (28204, Qiagen). DNA was then amplified using the GenomePlex Whole Genome

Amplification Kit (WGA2, Sigma). The samples were sequenced on Illumina NextSeq hardware and assessed for quality using FastQC (Andrews S. 2010, FastQC: a quality control tool for high throughput sequence data. Available online at: <http://www.bioinformatics.babraham.ac.uk/projects/fastqc>) or used for qRT-PCR analysis with the primers described before. Reads were trimmed using fastx-trimmer ([http://hannonlab.cshl.edu/fastx\\_toolkit/](http://hannonlab.cshl.edu/fastx_toolkit/)). Trimmed sequences were mapped to the GRCh38 version of the human genome with STAR 2.4.2a<sup>4</sup> using only unique alignments to exclude reads with unclear placing. PCR duplicates were removed using Picard 1.136 (Picard: A set of tools (in Java) for working with next generation sequencing data in the BAM format; <http://broadinstitute.github.io/picard/>) to avoid PCR artefacts leading to multiple copies of the same original fragment. Peaks were called using homer findPeaks version 4.03<sup>11</sup> with parameter –region to combine close peaks. The minimum distance and size of peaks were adjusted as followed: -size 2000 and –minDist 10000 for H3K9me3. To detect differential bound Peaks we applied homers getDifferentialPeaks with the parameters –F 1.4 and –P 0.000005. For Figure 4A, ChIP sequenced data were analyzed for H3K9me3 using Homer throughout the whole genome and the unique values for control and EndMT were summarized in methylation scores. These scores were then visualized with Circos software version circos-0.69-6. The highest H3K9me3 peaks from ChIP-sequencing were analyzed in detail using UCSC Genome Browser (Version: human Dec. 2013 (GRCh38/hg38) assembly and Repeat Masker program of Arian Smit on GRCh38.p12 version.

### **Animals**

All animal experiments were performed in accordance with the animal welfare guidelines and German national laws and were authorized by the competent authority (Regierungspräsidium Darmstadt, Hessen, Germany). C57BL/6J Jmjd2b<sup>f/f</sup> mice were obtained from Hitoshi Okada and already described.<sup>12</sup> Mice were crossed with C57BL/6J Cdh5-CreERT2 mice (obtained from the Jackson Laboratory) and treated with 2 mg/injection tamoxifen for 2 weeks (n=7-10; female and male, 10 weeks-old). After additional 2 weeks, left anterior descending (LAD) coronary artery ligation surgery induced myocardial infarction was performed.

### **Myocardial infarction (MI)**

MI was performed in 12 to 14 week old male and female Cdh5-iCre; Jmjd2b<sup>fl/fl</sup> mice. The animals were anesthetized with isoflurane and analgesia was delivered by an intraperitoneal injection of Buprenorphin (0.1 mg/kg body weight (BW)) in combination with a block of the intercostal nerves by using Bupivacaine (1 mg/kg BW, 0.25 % Bupivacaine). For postoperative analgesia, Buprenorphin and Caprofen (5 mg/kg BW) were given every 12 or 24 h for 3 days. Postoperative infections were prevented by giving Ampicillin (1 mg/10 g BW) in the drinking water. Under mechanical ventilation, the MI was induced by permanent ligation of the left anterior descending coronary artery (LAD). After 3 days post MI, the heart and the liver was harvested for single-cell RNA sequencing (heart) or for knockout check (liver), 14 days post AMI for immunohistochemistry. Echocardiography was performed on day 0, 7 and 14. Analysis was performed using the program VevoLab (Visualsonics) with Simpsons.

### **Isolation of liver endothelial cells (ECs):**

To check the knockout efficacy of Jmjd2b we isolated ECs from the liver. Mice were first perfused with GBSS (#G9779, Sigma), the lung was removed and dissociated with collagen type II (#17101-015 Gibco; 600 U/mice) using the GentleMACS. After 30 min at 37°C, cells were filtered with a 200 µm pore cell strainer and centrifuged at 290 x g, 10 min. The cell pellet was mixed with nycodenzsolution (35 %; #1002424 AXIS-SHILD) and overlaid with GBSS. After centrifugation without brake, cells were washed twice with cold MACS-Puffer (1 % FCS, 2 mM EDTA in PBS) and incubated with LSEC-Beads (#130092007 Miltenyi) for 30 min. Endothelial cells were then separated using a magnet based elution. RNA was isolated and expression was analysed using qRT-PCR with primers described before.

### **Immunohistochemistry (IHC)**

Mouse hearts 14 days post AMI were perfused with HBSS with Ca<sup>2+</sup> and Mg<sup>2+</sup> and fixed with 4% PFA. The hearts were embedded in paraffin and sectioned at 4 µm thickness using a microtome. Sections were incubated at 60 °C for 30 min, de-paraffinised and rehydrated. To analyse fibrosis, sections were incubated in 0.1 % Picro Siriusred F3BA solution for 1 h (Siriusred #1A280 Waldeck GmbH, Picric acid #6744.1GA Sigma

Aldrich), washed with acidified water, dehydrated and cleared with xylene. Siriusred staining intensity was measured using ImageJ, normalized to the total tissue.

For antibody stainings, sections were incubated in citratbuffer (pH 6, 0.1 M) and blocked with 5 % donkeyserum. Tissues were stained with S100A4 (1:100, #07-2274 Milipore), biotinylated Isolectin B4 (1:50, #B1205, Vector) and Hoechst 33342 (1:400, #AS83218 Ana Spec) followed by secondary antibody incubation (donkey anti-rabbit Alexa Flour 555, #A31572 Life technologies; SAV Alexa Flour 647, #S32357 Invitrogen, both 1:200). Imaging and analysis was performed blinded. The images were taken at the Zeiss LSM780 confocal microscope. Within the border zone, 1-2 images per section (total of 3 sections) with a distance of 200  $\mu$ m were taken. For EndMT analysis Lectin and S100A4 positive cell within the border zone regions were counted and normalized to total Lectin area.

### **Single cell RNA-Sequencing (scRNA-Seq)**

Cellular suspensions were loaded on a 10X Chromium Controller (10X Genomics) according to manufacturer's protocol based on the 10X Genomics proprietary technology<sup>13</sup>. HUVEC in vitro and murine scRNA-seq in vivo libraries were prepared using Chromium Single Cell 3' v2 Reagent Kit and Chromium Single Cell 3' v3 Reagent Kit, respectively (10X Genomics), according to manufacturer's protocols. Briefly, the initial step consisted in performing an emulsion where individual cells were isolated into droplets together with gel beads coated with unique primers bearing 10X cell barcodes, UMI (unique molecular identifiers) and poly(dT) sequences. Reverse transcription reactions were engaged to generate barcoded full-length cDNA followed by the disruption of emulsions using the recovery agent and cDNA clean up with DynaBeads MyOne Silane Beads (Thermo Fisher Scientific). Bulk cDNA was amplified using a Biometra Thermocycler Professional Basic Gradient with 96-Well Sample Block (98°C for 3 minutes; cycled 14x: 98°C for 15 s, 67°C for 20 s, and 72°C for 1 minute; 72°C for 1 minute; held at 4°C). Amplified cDNA product was cleaned with the SPRIselect Reagent Kit (Beckman Coulter). Indexed sequencing libraries were constructed using the reagents from the Chromium Single Cell 3' v2 and Chromium Single Cell 3' v3 Reagent Kits as follows: fragmentation, end repair and A-tailing; size selection with SPRIselect; adaptor ligation; post-ligation cleanup with SPRIselect; sample index PCR and cleanup with SPRI select beads. Library quantification and quality assessment was



performed using Bioanalyzer Agilent 2100 using a High Sensitivity DNA chip (Agilent Genomics). Indexed libraries were equimolarly pooled and sequenced using paired-end 26x98bp as sequencing mode by GenomeScan (Leiden, Netherlands). Single-cell RNA-Seq outputs were processed using the Cell Ranger (10X Genomics) suite versions 2.1.1 (in vitro HUVEC Control vs. EndMT samples) or 3.0.1 (in vivo 3d AMI samples, in vitro HUVEC JMJD2B knockdown samples). Both HUVEC in vitro datasets have been mapped to the GRCh38 (version 1.2.0) reference genome by using the “count” function. For HUVEC Control vs EndMT samples, individual processed datasets have been merged with “aggregate”. Secondary analysis was conducted using the Seurat 2.3.4 package in R.<sup>14</sup> We filtered the data for cells expressing at least 200 genes, as suggested by the distributor’s tutorial (satijalab.org). Moreover, we aimed to avoid doublets by removing cells with high unique molecular identifier (UMI) counts (> 90000) and high number of genes (> 8000). We also accounted for possible dead cells and removed cells with high mitochondrial content (> 10 % of total UMI). The remaining matrix was log-normalized and scaled. After detecting variable genes, a principal component analysis (PCA) using 10 dimensions was applied. Clustering of the cells was then performed by Seurat’s FindCluster function with 0.6 resolution. We used t-distributed stochastic neighbor embedding (t-SNE) to visualize cell clusters.<sup>15</sup> We applied a generic threshold of 2.5 to the scaled value of all candidate genes to separate high, low or no expressing cells.

HUVEC JMJD2B knockdown data has been analyzed with Seurat 3.0.2. We applied similar filters for removing cells with high and low UMI counts but removed the upper 5% and lower 1% of all cells per individual sample. High mitochondrial content cells (>10 %) were removed similarly. We aggregated the individual samples by using anchor-based integration methods as described in the Seurat 3 tutorial.<sup>16</sup>

Data were visualized by violin plots showing scaled and normalized RNA expression as implemented in Seurat’s *VlnPlot* function. Accordingly, in vivo 3d AMI data we mapped against the mm10 (version 3.0.0) reference genome using Cell Ranger “count”. In Seurat 2.3.4 we applied similar filters as for HUVEC datasets. We only kept genes that showed at least in 2 cells an UMI count of more than 1. We merged the data and counted cells expressing at least 1 UMI for *Cdh5* and *Pecam1* (ECs) as well as *Cdh5*, *Pecam1* and two mesenchymal markers (EndMT cells) between the libraries. We used a

$\chi^2$ -statistic with contingency tables to calculate significant changes in the distribution. RNA expression changes of mesenchymal markers in all cells of both libraries were calculated with Seurat's *FindMarker* function, using the bimodal maximum likelihood test, as described by the online tutorial.

### **Statistics**

Mann–Whitney U-test or Student's t-test was used to test for statistical differences between two groups as appropriate. For more group's ANOVA with Dunnett's multiple comparison test was used. A value of  $P < 0.05$  was considered statistically significant. To test potential associations, Pearson's correlation were calculated. Significance for differential gene expression between the conditions in scRNA-Seq analysis was calculated with a bimodal maximum likelihood ratio test and  $\chi^2$ -statistic with contingency tables to calculate significant changes in the distribution, suitable for single-cell data. Microsoft Excel and GraphPad Prism 6 were used to calculate statistical differences.

### **Data availability**

The RNA-Sequencing, ChIP-Sequencing and Single-cell RNA Sequencing data will be deposited in the Gene Expression Omnibus database with the identifier "GSE143148". The microarray data are deposited in the Gene Expression Omnibus database with the identifier "GSE143150".

### **Supplemental References**

1. Hatch, S. B. *et al.* Assessing histone demethylase inhibitors in cells: lessons learned. *Epigenetics Chromatin* **10**, 9 (2017).
2. Boeckel, J.-N. *et al.* Jumonji domain-containing protein 6 (Jmjd6) is required for angiogenic sprouting and regulates splicing of VEGF-receptor 1. *Proc. Natl. Acad. Sci. U. S. A.* **108**, 3276–81 (2011).
3. Boeckel, J. N. *et al.* Identification and Characterization of Hypoxia-Regulated Endothelial Circular RNA. *Circ. Res.* **117**, 884–890 (2015).
4. Dobin, A. *et al.* STAR: ultrafast universal RNA-seq aligner. *Bioinformatics* **29**, 15–21 (2013).
5. Trapnell, C. *et al.* Transcript assembly and quantification by RNA-Seq reveals unannotated transcripts and isoform switching during cell differentiation. *Nat.*

- Biotechnol.* **28**, 511–5 (2010).
6. Michalik, K. M. *et al.* Long noncoding RNA MALAT1 regulates endothelial cell function and vessel growth. *Circ. Res.* **114**, 1389–97 (2014).
  7. Doddaballapur, A. *et al.* Laminar Shear Stress Inhibits Endothelial Cell Metabolism via KLF2-Mediated Repression of PFKFB3. *Arterioscler. Thromb. Vasc. Biol.* **35**, 137–145 (2015).
  8. Nam, D. *et al.* Partial carotid ligation is a model of acutely induced disturbed flow, leading to rapid endothelial dysfunction and atherosclerosis. *Am. J. Physiol. Circ. Physiol.* **297**, H1535–H1543 (2009).
  9. Gellert, P., Uchida, S. & Braun, T. Exon Array Analyzer: a web interface for Affymetrix exon array analysis. *Bioinformatics* **25**, 3323–4 (2009).
  10. Schmidl, C., Rendeiro, A. F., Sheffield, N. C. & Bock, C. ChIPmentation: fast, robust, low-input ChIP-seq for histones and transcription factors. *Nat. Methods* **12**, 963–5 (2015).
  11. Heinz, S. *et al.* Simple combinations of lineage-determining transcription factors prime cis-regulatory elements required for macrophage and B cell identities. *Mol. Cell* **38**, 576–89 (2010).
  12. Kawazu, M. *et al.* Histone Demethylase JMJD2B Functions as a Co-Factor of Estrogen Receptor in Breast Cancer Proliferation and Mammary Gland Development. *PLoS One* **6**, e17830 (2011).
  13. Zheng, G. X. Y. *et al.* Massively parallel digital transcriptional profiling of single cells. *Nat. Commun.* **8**, 14049 (2017).
  14. Butler, A., Hoffman, P., Smibert, P., Papalexi, E. & Satija, R. Integrating single-cell transcriptomic data across different conditions, technologies, and species. *Nat. Biotechnol.* **36**, 411–420 (2018).
  15. Mahfouz, A. *et al.* Visualizing the spatial gene expression organization in the brain through non-linear similarity embeddings. *Methods* **73**, 79–89 (2015).
  16. Stuart, T. *et al.* Comprehensive Integration of Single-Cell Data. *Cell* **177**, 1888–1902.e21 (2019).

